The degradation of nitrocellulose (NC) was investigated by looking at the explored degradation routes in alternative nitrate esters, and tested for NC a truncated model for the wider polymer It was found that the most suitable model for study of the key degradation reactions was a β-glucopyranose monomer, bi-capped with methoxy groups. This was determined via analysis of the quantum theory of atoms in molecules (QTAIM) bonding critical point (BCP) between the capping groups and the wider monomer, when changing from hydroxyl and methoxy homogeneous or mixed groups at the C1 and C4 sites on the ring. The model was nitrated at the C2 position, to mimic the first site of nitration or last site of denitration.

Contents

Abbreviations

ψ	wavefunction
%N	percentage nitrogen by mass
2-NDPA	2-Nitrodiphenylamine
a.u.	atomic units
B3LYP	Becke, 3-parameter, Lee-Yang-Parr hybrid functional
BCP	bonding critical point
CH_3CH_3	NC repeat unit with two $-OCH_3$ capping groups
CH_3OH	NC repeat unit with $-OCH_3$ capping group on ring 1, $-OH$ group on ring 2
CCP	cage critical point
CP	critical point
DFT	density functional theory
DSC	differential scanning calorimetry
DOS	degree of substitution
DPA	diphenylamine
EM	energetic materials
EN	ethyl nitrate
ESP	electrostatic potential

G09 Gaussian 09 revision D.01

GM genetically modified

GView Gauss View 5.0.8

HF Hartree Fock theory

IR infra-red spectroscopy

MEP minimum energy path

MM molecular mechanics

MMFF94 Merck molecular force field 94

MP2 Møller–Plesset perturbation theory with second order correction

MW molecular weight

NC nitrocellulose

NCP nuclear critical point

NG nitroglycerine

NMR nuclear magnetic resonance spectroscopy

$OHCH_3$ NC repeat unit with $-$OH capping group on ring 1, $-OCH_3$ group on ring 2

PCM polarisable continuum model

PES potential energy surface

PETN pentaerythritol tetranitrate

PETRIN pentaerythritol trinitrate

QM quantum mechanics

QTAIM quantum theory of atoms in molecules

RCP ring critical point

SB59	1,4-bis(ethylamino)-9,10-anthraquinone dye
SEM	scanning electron microscopy
S_N2	bi-molecular nucleophilic substitution reaction
TG	thermogravitmetric analysis
TS	transition state
UFF	universal force field
UV	ultraviolet
UVvis	ultraviolet–visible spectroscopy
ωB97X-D	ωB97X-D long-range corrected hybrid functional
ZPE	zero-point energy

Chapter 1

Mechanisms of denitration

1.1 Introduction

The first stage of thermolytic decomposition for nitrate esters is generally agreed to be homolytic fission of the O-N bond linking the nitrate to the alkyl chain, leading to the loss of $^{\cdot}NO_2$ (equation 1.1) [1, 2, **?**] Though nitrate homolysis is an endothermic reaction, the weak O-N bond has a typical dissociation enthalpy of 42 kcal mol^{-1} and is easily cleaved when exposed to elevated temperatures, UV light or impact. Whilst the thermolytic degradation of energetic materials has been widely studied experimentally, the ambient, slow ageing mechanisms are less well documented. Low-temperature decomposition routes are influenced by many factors over a protracted lifetime, and in practical use, materials are usually subject to evolving environmental conditions. External changes in pressure, humidity, stress and temperature cycles induce variation in the degradation patterns of energetic materials. The presence of moisture has been observed to lower the activation energy and accelerate the decomposition of energetic materials [2]. Internal factors including impurities and residual solvent, and crystal growth within the bulk, also alter decomposition behaviour.

$$R{-}ONO_2 \longrightarrow R{-}O^{\cdot} + {}^{\cdot}NO_2 \tag{1.1}$$

$$R{-}ONO_2 \longrightarrow R{=}O + HNO_2 \tag{1.2}$$

The decomposition of nitrate esters at temperatures over 100°C is dominated by thermolytic processes, whilst under 100°C, decomposition is thought to largely be the result of hydrolysis [3]. Tsyshevsky *et al.* studied the intramolecular reactions leading to denitration in pentaerythritol tetranitrate (PETN) in both the vacuum and the bulk crystal [4] (figure 1.1). It was found that the two dominating decomposition reactions were homolysis (equation

1. $^{\cdot}NO_2$ loss
2. HNO_2 loss
3. OONO rearrangement
4. γ-attack
5. $ONO_2^{\cdot}$ loss
6. C−C cleavage ($CH_2O + NO_2$)
7. C−C cleavage ($CO + HNO_2$)

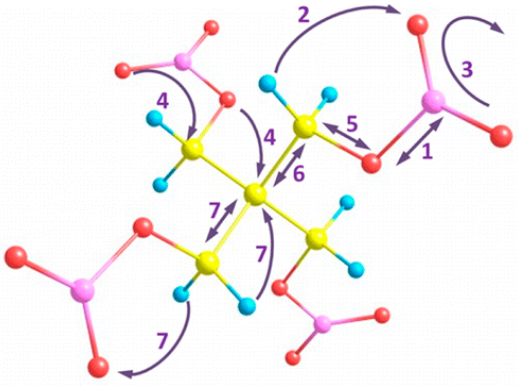

Figure 1.1: Intramolecular thermolytic reactions in PETN, from the work of Tsyshevsky *et al.* [4].

1.1) and intramolecular elimination of HNO_2 (equation 1.2). Whilst elimination of HNO_2 was found to be the most energetically favourable denitration pathway, homolytic fission dominated preliminary decomposition steps due to the lower activation barrier and faster rate of reaction. It was suggested that global decomposition processes were determined by the interplay between the two mechanisms. Initial homolysis facilitated wide-spread denitration, complemented by exothermic HNO_2 elimination promoting self-heating of the system and further bond dissociations. The presence of $^{\cdot}NO_2$ and HNO_2 were previously linked to autocatalytic rates observed for later-stage decomposition of nitrate esters [5, 6, 7, **?**], though some studies solely attribute it to the presence of acids [8, 9, 10, 11]. However, from these initial processes it is not possible to determine which is the species resposible

Spent acids remain in the NC matrix following synthesis even with thorough washing procedures. Acids are further generated via the subsequent reactions of $^{\cdot}NO_2$ following homolysis. The acidic species proceed to react with other moieties in the system, such as unsubstituted alcohol side chains on the polysaccharide, or other small molecules free in the bulk.

When exploring the interaction of nitroglycol and nitroglycerin in acid solution, Camera proposed a protonation-denitration scheme whereby initial protonation at the nitrate is rapid, but subsequent release of the nitronium ion was slow (scheme 1.1).

NC in storage is kept wetted with solvents to prevent drying and self-ignition. Material with 12.6%N or lower, must be stored in 25% water by mass, or a mixture of solvents and plasticisers. In the study of organonitrates and organosulfates generated from isoprene

$$CH_3CH_2ONO_2 + H^+ \overset{\text{fast}}{\rightleftharpoons} CH_3CH_2ONO_2H^+ \quad (1.3)$$

$$CH_3CH_2ONO_2H^+ \overset{\text{slow}}{\rightleftharpoons} CH_3CH_2OH + NO_2{}^+ \quad (1.4)$$

Scheme 1.1: The relative rate of stepwise protonation and denitration of nitrate esters, using ethyl nitrate as an example. From the work of Camera *et al.* [12].

as secondary organic aerosols, Hu *et al.* found that primary and secondary nitrates were resilient to hydrolysis for pH > 0, whilst tertiary nitrates underwent hydrolytic nucleophilic substitution easily, reacting with water to form alcohols [13]. Primary nitrates are those

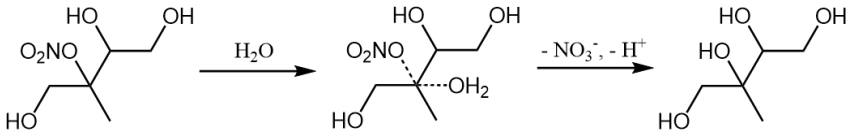

Scheme 1.2: Hydrolysis of a tertiary nitrate derived from the reaction of isoprene in the aerosol phase, from the work of Hu *et al.* [13].

with one non-hydrogen moiety on the carbon, (additional to the nitrate linkage) with the remaining two bonds linked to hydrogens. Secondary nitrates are those where the nitrate carbon posses one bonded hydrogen atom, and two further non-hydrogen moieties. In tertiary nitrates, the carbon is fully substituted with no attached hydrogens. This latter group is usually sterically hindered and stabilising to carbocations, condition on the other substituents. If formation of a carbocation intermediate is involved in the hydrolysis mechanism, this may explain why the tertiary nitrates exhibited highly efficient denitration, even under neutral conditions.

Though no specific mechanistic detail is given, the action of a protonated transition state during hydrolysis is alluded to by Hu *et al.*, through the contrast between the rate of acid-catalysed and neutral hydrolysis reactions. Neutral hydrolysis of the tertiary nitrates occured rapidly, but hydrolysis only occurred for primary and secondary nitrates under strongly acid catalysing conditions at much lower rate. It was found that the presence of adjacent OH groups hampered the rate of hydrolyis for some aerosol dispersed organonitrates. In the neutral hydrolysis of tertiary nitrates, increasing the number of adjacent OH groups lead to protracted hydrolysis lifetimes. Interestingly, the retardation effect of adjacent OH groups was not observed for the the acid catalysed cases. Hu proposed that this could be due to the interaction of OH with the transition state of the neutral hydrolysis

system, compared to the protonated transition state of the acid catalysed system, impeding the reaction only in the former case. There is evidence that nitration and denitration of nitrate esters is also influenced by the presence of nitrate groups at neighbouring positions. Matveev *et al.* demonstrated that for poly-nitroesters the rate of liquid-phase decomposition did not increase linearly with number of nitrate reaction centres. It was found to mainly dependend on individual structures (table 2.2) [14].

It was suggested that the trend in reactivity could be partially explained by the inductive effect of the nitro groups [1]. The inductive effect arises when a difference in the electronegativity between atoms connected by a σ bond leads to a polarisation, or permanent dipole, in the bond. Electron donating groups increase the δ- partial charge on neighbouring atoms through the release of electrons, whilst electron withdrawing groups pull electron density away from neighbouring atoms generating a δ+ charge on connected atoms. However, the π donation by lone pairs on the oxygen and nitrogen plays a significant role in increasing electron density of neighbouring atoms, known as the resonance effect. NO_3 presents a stronger electron donating effect via π donation than OH. It would therefore be expected that both increase the rate of hydrolysis for nearby leaving groups. The presence of an adjacent nitrate appears to facilitate denitration, whereas the presence of hydroxyl groups hinders this process, for neutral hydrolytic schemes. This suggests that the proposed interaction of the hydroxyl group with the neutral transition state supersedes its resonance effect. As a result,

Table 1.1: Comparison of rate constants of decomposition for various polynitrate esters at 140°C. Collated from literature sources by Matveev *et al.*[14]. ΔT is the decomposition temperature range, E is the experimental activation barrier for decomposition, log$A$ is the pre-exponential factor, T_c is the combustion temperature, k_{expt} is the rate constant for decomposition.

Compound	ΔT / °C	E / kcal mol^{-1}	log$A$ [s^{-1}]	k_{expt} / 10^{-6} s^{-1}
$O_2NOCH_2CH_2CH_2ONO_2$	72–140	39.1	14.9	1.7
$O_2NOCH_2CH_2CH_2CH_2ONO_2$	100–140	39.0	14.7	1.1
$O_2NOCH(CH_3)CH(CH_3)ONO_2$	72–140	40.3	14.9	5.0
$O_2NOCH_2CH_2OCH_2CH_2ONO_2$	80–140	42.0	16.5	1.9
$O_2NOCH_2CH(OH)(CH_2ONO_2)$	80–140	42.4	16.8	2.3
$O_2NOCH_2CH(ONO_2)(CH_3)$	72–140	40.3	15.8	3.0
$[(O_2NOCH_2)CH(ONO_2)CH(ONO_2)]_2$ (hexanitromannite)	80–140	38.0	15.9	63.0

it is ambiguous whether any apparent rate increase due to the presence of adjacent nitrate groups arises as a result of the resonance effect of the nitrate, or whether it is solely due to the absence of a neighbouring hydroxyl.

The investigation by Hu *et al.* exclusively focused on nitrates generated from an isoprene precursor, upon dispersion as an aerosol. The nitrate groups present in NC are either of primary (C6) or secondary (C2, C3) structure, indicating that ambient hydrolysis is unlikely according to this scheme. However, solvent effects are expected to differ for condensed-phase reactions and aerosol phases. A greater build-up of acid concentration can be achieved in a closed, condensed system, and the lifetime of an aerosol is relatively short-lived when considering the timescale of slow ageing processes in NC. Thus, the work of Hu *et al.* does not provide a direct comparison for the NC polymer but highlights the the possible contribution from both neutral and acid-catalysed hydrolysis routes and of increasing levels of substitution on the wider structure.

In this section, the possible mechanisms for nitrate removal from the NC backbone are explored. The homolytic fission and HNO_2 elimination thermolytic processes suggested by Tsyshevsky will be compared to the acid hydrolysis scheme. Though the relative rates of reaction were not compared, the extended timescales involved in ambient ageing imply that the dominating reactions correspond to those most thermodynamically favourable.

1.2 Methodology

The energies of homolytic fission and elimination of HNO_2 were calculated for PETN, as a test system before extension to the monomer. The reaction energies were calculated according to equations 1.1 and 1.2 to reproduce the work of Tsyshevsky *et al.*. The literature geometries of PETN and its derivatives were obtained from the authors. A single point energy and frequency calculation were performed on each of the relevant structures to determine the reaction energies; no geometry optimisation was performed on the given structures except for in the case the $^{\cdot}NO_2$ molecule, where the geometry was not given.

The intramolecular reactions of the NC monomer were modelled according to scheme 1.3. Rigid and relaxed potential energy surface (PES) scans were attempted in order to locate transition states for both reactions for the NC monomer. Where the scans were unable to identify a valid transition state geometry, guess transition state geometries were constructed and optimised.

The possible protonation sites for the NC monomer were explored by placing a proton

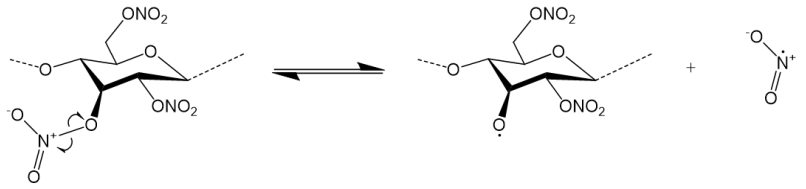

(a) Removal of a nitrate group *via* homolytic fission of NC

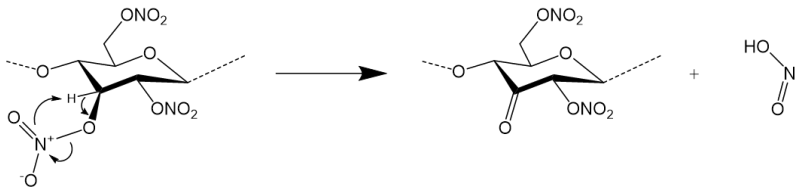

(b) Removal of a nitrate group *via* elimination of HNO_2.

Scheme 1.3: The proposed intramolecular reactions for the initial denitration step during NC degradation.

at each of the different oxygen sites surrounding the nitrate group. The structures were then geometry optimised and energies of protonation were compared. H_3O^+ was modelled as the donating species; as NC is usually stored wetted in water, the hydronium ion is the most likely source of protons. It is also possible that the proton is donated by other acidic species in the system, particularly HNO_2 or HNO_3. This is more likely at later stages of degradation when a higher concentration of acid has been generated by secondary reactions.The effects of tunneling were not accounted for.

1.2.1 Computational details

All geometry optimisation, thermochemistry calculations and PES scans were performed in Gaussian 09 revision D.01 (G09). Geometry optimisation and thermal calculations were to the level of 6-31+G(2df,p). NC monomer structures were optimised using ωB97X-D long-range corrected hybrid functional (ωB97X-D), Becke, 3-parameter, Lee-Yang-Parr hybrid functional (B3LYP) and Møller–Plesset perturbation theory with second order correction (MP2). ΔG values were obtained by the difference between the thermally corrected free energies of products and reactants. Zero-point corrected energies ZPE were determined by addition of individual zero-point energy (ZPE) to the free energy:

$$\Delta G^{ZPE} = \sum(G_{products} + ZPE_{products}) - \sum(G_{reactants} + ZPE_{reactants}) \tag{1.5}$$

PES scans were performed to the level of ωB97X-D/6-31+g(d), or using unrestricted ωB97X-D, in the case of $O-{}^{\cdot}NO_2$ dissociation. Rigid scans were carried out by fixing

bond lengths, angles and dihedral values as constants. Only the variable of interest was allowed to change, with the exception of relaxation of other specified coordinates required for accommodation of the new geometry, following each step of the scan. For example, in the homolysis of the nitrate $O-NO_2$ bond, as the NO_2 group departed, the internal O–N–O angle was also allowed to relax, in addition to the angle of the departing NO_2 with respect to the remainder of the molecule. In two-dimensional scans, two variables are scanned. For the same reaction, the elongation of a the $O-NO_2$ bond was scanned with simultaneous approach of a proton, to monitor the effect of protonation for the same reaction. Relaxed scans were performed in Gaussian using the 'modredundant' function, whereby the whole structure was geometry optimised after each step of the scan. Scans were performed with step size of 0.1 Å. The number of steps varied with the property investigated, though the majority of the phenomena were observed within 20 steps (2 Å). Scans were attempted in vacuum, and for some cases, polarisable continuum model (PCM) implicit solvent [15].

1.3 Results and discussion

1.3.1 Thermolytic decomposition mechanisms

The energies of homolytic fission and intramolecular elimination of HNO_2 from a PETN nitrate group are shown in table 1.2. The energy values calculated by Tsyshevsky *et al.* are denoted in parenthesis. Despite using the supplied geometries, same method and basis, it can be seen that the reaction energies obtained for PETN vary greatly from the values found by Tsyshevsky *et al.*. Inspection of the forces showed that they were in fact not converged. It was expected that the given geometries were used to generate the reaction energy values quoted in the study. The unconverged structures therefore do not fully explain the large discrepancy between the literature energies and obtained values here. A small contribution may arise from a different compilation of the G09 program, leading to fluctuations in the exact values obtained which are amplified when deriving reaction energies.

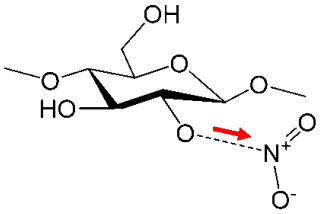

Figure 1.2: The $O-NO_2$ bond was elongated during rigid and relaxed PES scan to simulate homolytic fission for the NC monomer.

Table 1.2: Calculated free energies of reaction (ΔG_r), reaction enthalpies (ΔH_r), activation barriers (E_a) with zero-point correction (^{ZPE}) for the intramolecular reactions of PETN, and the NC monomer. Values expressed in kCal mol^{-1}.

Reaction	ΔG_r	ΔG_r^{ZPE}	ΔH_r	E_a	$E_a{}^{ZPE}$
PETN					
$^{\cdot}NO_2$ loss	21.51 (41.2)[a]	16.56 (35.8)	35.62	21.51[b] (41.2)	16.56 (35.8)
HNO_2 loss	−23.63 (−18.6)	−26.21	−20.39	41.29 (47.3)	36.28 (42.7)
NC monomer					
$^{\cdot}NO_2$ loss	23.25	18.69	36.26	23.25	18.69
HNO_2 loss	−36.05	−39.42	−22.86	40.70	37.33

[a] values from the work of Tsyshevsky *et al.* [4].
[b] values for the activation energy and total energy of reaction are the same for bond dissociation via homolytic fission.

what scans did I do for HNO2? Get a pic of the transistion state.

The energy profile of homlytic fission was obtained via PES scans of NO_2 leaving the NC monomer. The internal angle of the departing NO_2, in addition to the coordinates referencing its orientation relative to the rest of the molecule, was allowed to relax. As the scan progressed the NO_2 internal angle increased from 129.2 °to 134.0 °at a maximum separation of 3.4 Åfrom the bridging oxygen (Ox), corresponding to the formation of a $^{\cdot}NO_2$ radical (internal angle 134.3 °).

1.3.2 Acid hydrolysis mechanism

1.3.2.1 Protonation site

The protonated NC monomer species are shown in figure 1.3. The bridging oxygen (Ox) linking the nitrate to the remainder of the molecule, the capping group oxygen, and the interchangeable terminal nitrate oxygen sites were protonated in order to compare their relative energies for determination the site most likely to stabilise the proton at thermal equilibrium. Protonation also occurs on other sites in the molecule, such as at unsubstituted hydroxyl groups, the capping group oxygen on C4 and O1 in the glucose ring. Though is a possibility that protonation at further sites in the monomer would contribute to degradation processes *via* alternative mechanisms, for the purposes of studying denitration via acid hydrolysis, only the sites peripheral to the nitrate leaving group were explored. The

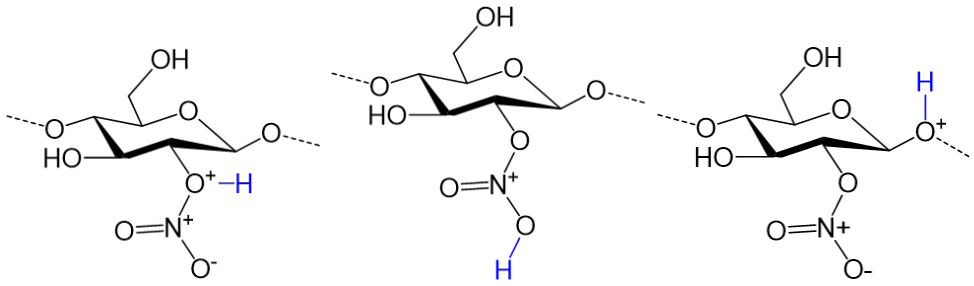

Figure 1.3: Protonation sites on the NC monomer for hydrolysis of the nitrate at the C2 position.

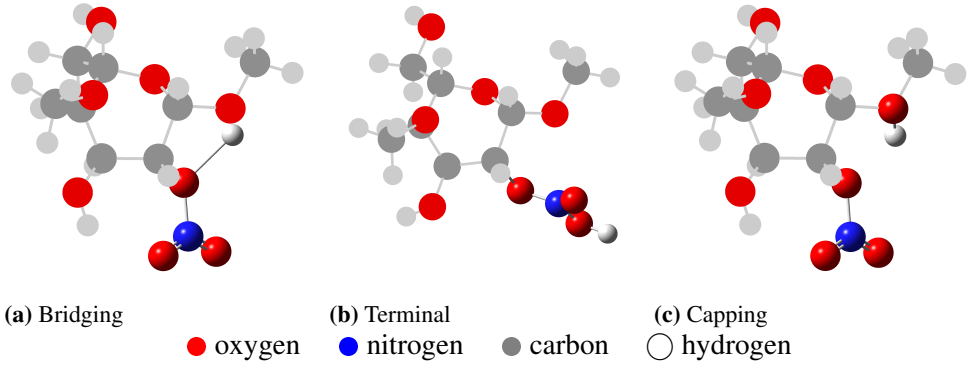

Figure 1.4: Optimised protonated NC monomer structures, showing interaction between the proton on the bridging site with the capping group oxygen.

mechanism of protonation was not explored in depth here; it was assumed that the protons in the system would be in fast exchange between the molecule and the solvent. The process has been studied computationally by Jebber *et al.* and Liu *et al.* [**?**, **?**]. The optimisation of water as a protonating species was attempted, to see whether it was possible to stabilise in coordination. The optimisation of H3O in coord with fully nitrated monomer was also tested, but was only possible up to the level hf/6-31g. Evaluation of the energy of protonation at each site found that the bridging

Big table of all the scans I did (for hydrolysis TS)

Columns:

Table 1.3: Free energies of protonation at each of the oxygen sites of interest on NC repeat unit with two $-OCH_3$ capping groups (CH_3CH_3) C2 monomer of NC.

Protonation site	ΔG_r /kcal mol^{-1}			
	ωB97X-D	PCM	B3LYP	PCM
Bridging	−30.88	0.85	−31.99	−0.25
Terminal	−23.13	10.00	−24.06	10.97
Capping	−30.43	0.85	−31.98	0.64

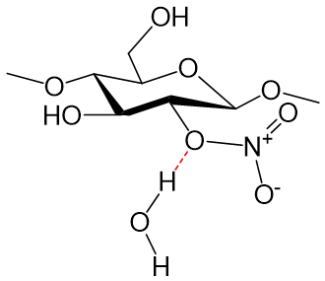

Scanned co-ordinate. Distance scanned. Observation. (TS found? etc)

1.3.3 Denitration by hydrolysis

Following the protonation step, possible transition states for the removal of the nitrate were investigated. A PES scan was performed on the NC monomer protonated at the bridging site, where the O−NO_2 bond was elongated in order to determine whether the NO_2 is lost, leaving the hydroxyl group as expected. Unrestricted ωB97X-D was used, with 20 steps of 0.1 Å, however bond dissociation was not observed even when extending the scan distance to a maximum of 6.4 Å. Instead, a steady increase in the energy was observed.

The PES scan of NO_2 removal from ethyl nitrate protonated at the bridging site was used as a preliminary test for the mechanism of denitration following protonation. 4-membered ring and 6-membered ring structures were optimised in order to determine

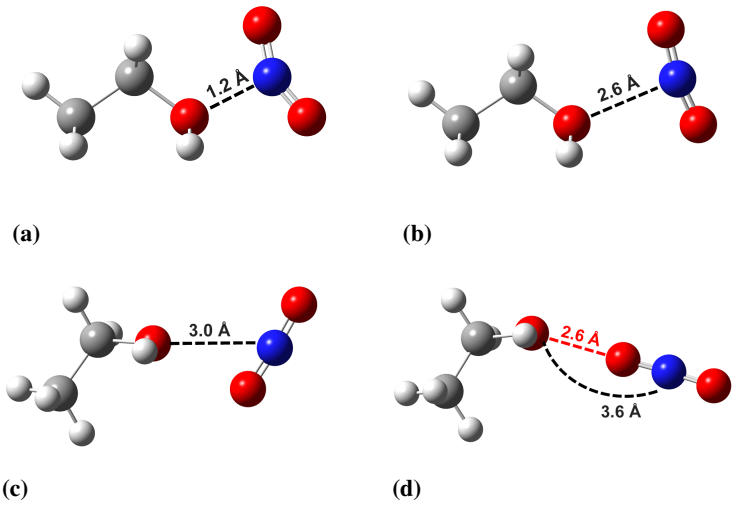

Figure 1.5: Geometries from steps 1, 7, 11 and 26 of the PES scan of ethyl nitrate (EN)

whether they were energetically and geometrically feasible. It can be seen that as the nitrate departs, it aligns with the hydroxyl group in an orientation suitable for formation of a peroxy

group. Optimisations were attempted with both full geometry relaxation, and various frozen

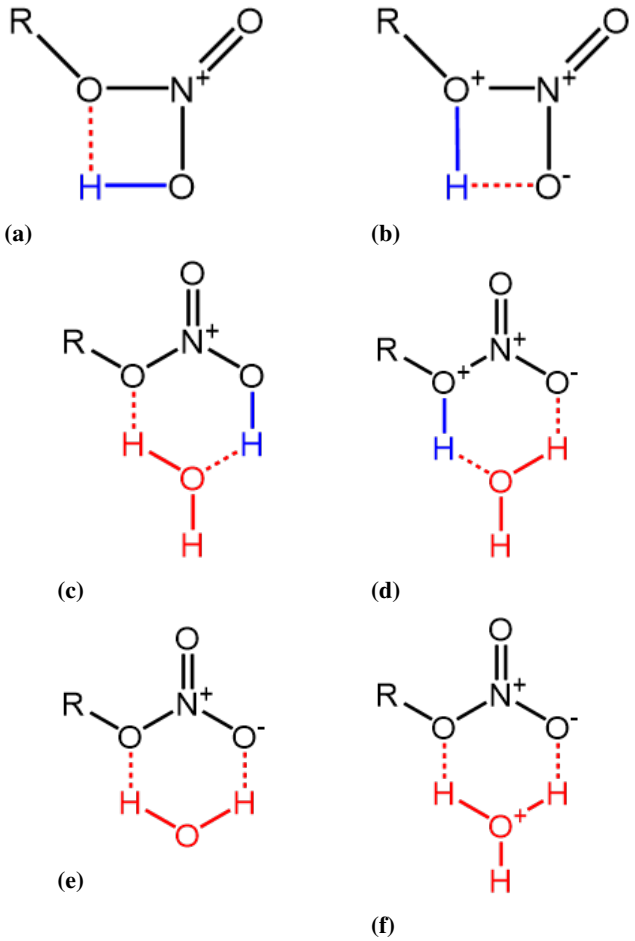

Figure 1.6: Proposed 4-member and 6-member ring transition states for the denitration of a nitrate ester, under various hydrolytic conditions. R = CH_3 in the case of methyl nitrate, R = CH_2CH_3 in the case of ethyl nitrate and R = $(H_3CO)_2C_6H_9O_3$ for the monomer.

co-ordiate schemes; fixing of the bulk molecule with relaxation only around the nitrate and co-ordinating species or relaxation of the wider molecule with fixed coordinates around the nitrate. Fully relaxed structures did not show convergence. It was possible to optimise the 4-membered ring bridging transition state with frozen ring geometry and relaxation of the remaining molecule (figure 1.6b). A rigid scan of the 4-membered ring transition starting from the bridging protonation site revealed that as the nitrate moved away from the system, the proton moved to the capping group site rather than remain on the bridging oxygen as a hydroxyl, as was expected. Instead a ketone group was formed between the bridging oxygen and the ring. At subsequent steps, the ketone group causes the C2 - C3 bond to elongate and break. The scan eventually revealed the NO_2 leaving group reclaiming the proton from the capping group oxygen, leading to ring fission.

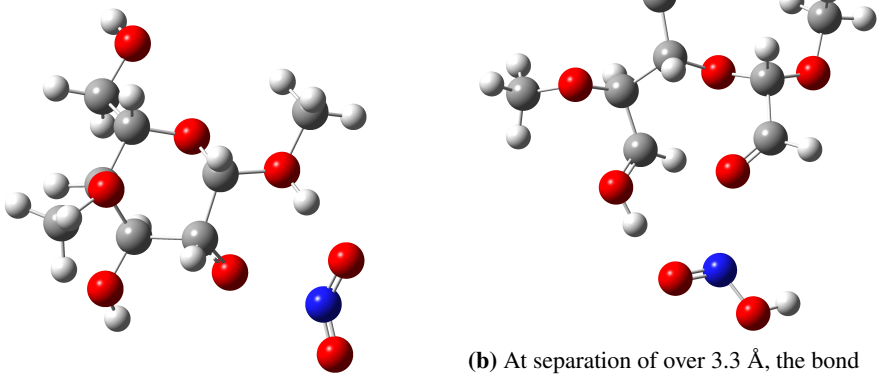

(a) In the initial stages of increasing O−NO_2 distace, the proton moves to the capping group.

(b) At separation of over 3.3 Å, the bond between C2 an C3 breaks, leading to ring fission. The proton then eventually moves back onto NO_2 .

Figure 1.7: Relaxed scan of NO_2 departure, starting with the 4-membered ring structure.

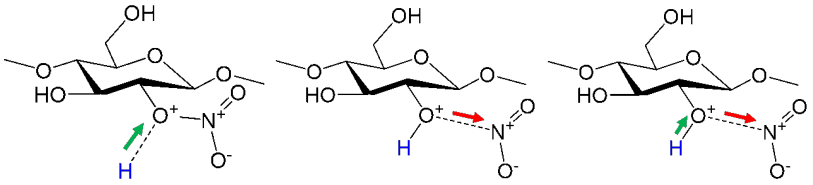

Figure 1.8: The scanned coordinates.

Things I did:

4 membered ring

–Scan using ethyl nitrate

–Opt Ts using ethyl nitrate

–considerations - sterics, and what energy barrier would be required to overcome the twist needed to obtain this state. Orbital overlaps?

6 membered ring

–considerations - sterics, and what energy barrier would be required to overcome the twist needed to obtain this state. Orbital overlaps?]

–Would energetics allow you to skip the protonation step? Is it more favourable?

C2 and water

Still to mention:

- Compare the results from different methods - which were the best for describing the reactions? - Theoretical aspects to the above lines of arguement.

1.4 Summary

Homolysis is fastest, for the monomer too, with HNO2 coming in second due to slower rate / energetics. (Check if I did anything to actually find this out - may just have to compare energetics.) Scans did confirm that $^{\cdot}NO_2$ left as a radical. Scans showed the energy profiles involved (again, was HNO2 ever seen to be formed?)

AH rate was not able to be compared as a TS was not found. Protonation occurs on both terminal and bridging sites of the monomer, with location at the bridging site conducive to the removal of NO_2^+.

TS were not able to be isolated for the denitration step, even with coordination with water in different orientation and both 4 and 6 mem ring TS. 2D scans did reveal a possible TS but it did not lead to the desired denitration pathway. See water clusters around NC by [16].

Chapter 2

Post-Denitration Reactions

2.1 Introduction

Products of the preliminary denitration step of NC can be evolved as gases or remain trapped in the polymer matrix. Reactive nitrogen dioxide radicals generated from homolysis of the O-N bond are likely to migrate within the bulk and attack other sites on the polysaccharide, initiating branched radical chain reactions. These lead to deeper decomposition of the polymer *via* chain scission and rupture of glucose rings, with eventual complete disintegration of the molecule, assisted by products released by ongoing acid hydrolysis. Nitrous and nitric acids are released directly from denitration or via transformation of released NO_x species. In addition to catalysing hydrolysis, they increase the acidity of the overall system, lowering the pH and stimulating further hydrolytic processes [13]. The final product mixture is dictated by the numerous side reactions involving autocatalysis, radical reactions and product interactions.

When studying the ageing of NC using UVvis spectroscopy, Moniruzzaman *et al.* observed increasing concentrations of reaction products beyond those generated from first-stage decomposition, following heat treatment over extended timescales [17, 3]. The reaction of the 1,4-bis(ethylamino)-9,10-anthraquinone dye (SB59) with NO_x released by denitration, mimics the action of stabilisers such as diphenylamine (DPA) and 2-Nitrodiphenylamine (2-NDPA) commonly used in NC formulations. The secondary amine groups of the dye consume any nitrates in the system, eliminating the possibility of successive reactions generating acidic species. Un-aged NC thin films, and films aged at 40°C, 50°C, 60°C and 70°C for timescales of up to 2000hrs for 40°C, were compared. UV absorbances at 600 nm and 650 nm were characteristic of the SB59 dye used to indicate the presence of NO_x, released by the denitration of NC (figure 2.2). The isosbestic point iden-

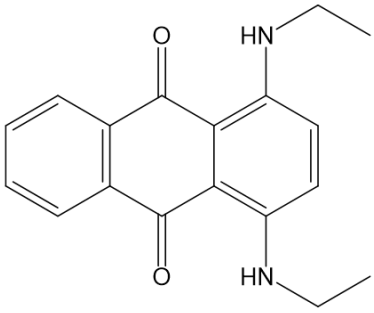

Figure 2.1: 1,4-bis(ethylamino)-9,10-anthraquinone dye (SB59) used to probe the release of nitrates from NC using ultraviolet–visible spectroscopy (UVvis) and ^{1}H NMR spectroscopy [3]. The action of nitrate absorption by the dye imitates that of stabilisers commonly used with nitrate ester formulations.

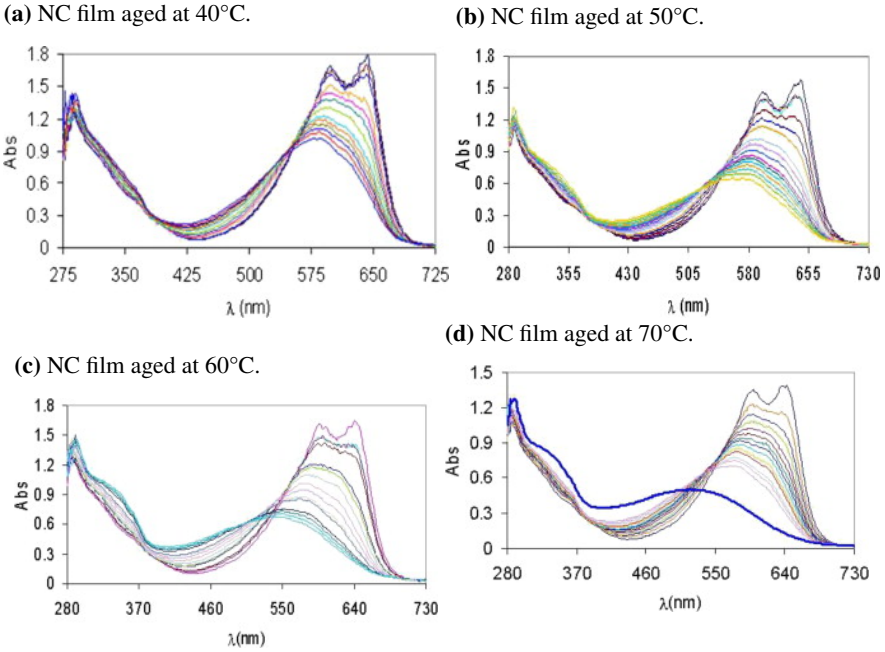

Figure 2.2: UVvis spectra of aged NC-based film, from the work of Moniruzzaman *et al.*[3]. The peaks at 600 nm and 650 nm are attributed to the π - π* transitions in the anthraquinone dye (SB59). Spectral lines with highest absorbance peaks in this region correspond to the sample prior to heat treatment. Peaks below 400 nm indicate the formation of SB59 derivatives due to secondary reactions.

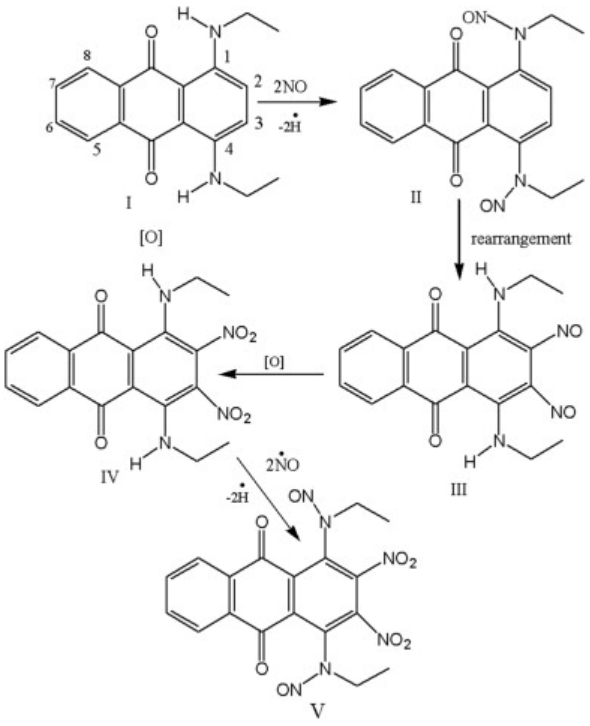

Figure 2.3: Proposed pathway for the reaction of SB59 dye with ·NO released as a result of denitration of NC [3].

tified at 552 nm showed a proportional relationship between the concentration of SB59 as it decreased, with the concentration of the [SB59 + NC] product as it increased. Samples exposed to higher ageing temperatures presented spectra dominated by products formed *via* secondary reactions. For samples aged at temperatures >40°C, the isosbestic point demonstrated a downwards shift with increasing dye consumption. In the case of the 70°C treated run, the final measurement (indicated by the royal-blue line in bold in figure 2.2d)) deviated from the isosbestic point entirely, with more than 81% consumption of the original dye concentration. The drift from the isosbestic point, in addition to the appearance of new absorbance peaks below 400 nm, allude to the presence of new species in the reaction mixture not generated by the primary reaction of SB59 and NC. It is likely that these arise from the continued reaction of SB59 derivatives with NC degradation products, or further derivatives thereof, as suggested in figure 2.3. Following cleavage of the nitrate ester via homolytic fission, elimination of nitrous acid, or hydrolysis, the resulting residues available for further reaction with the polymer or other free molecules in the system. In the study of PETN ageing at high temperatures (115 °C - 135 °C) in vacuum, and low temperatures (20 °C - 65 °C) in acetonitrile solution, Shepodd *et al.* commented that thermolysis produced a more complex and varied mixture, due to deeper degradation and recombination of radicals [**?**]. By

Thermolytic initiation

$$R{-}ONO_2 \longrightarrow R{-}O^{\cdot} + {}^{\cdot}NO_2 \tag{2.1}$$

Propagation

$$\begin{aligned} R{-}O^{\cdot} + {}^{\cdot}NO_2 \xrightarrow{R-ONO_2} & R{-}ONO_2 + {}^{\cdot}NO + {}^{\cdot}NO_2 + N_2O_4 \\ & + H_2O + N_2O + CO_2 + CO \\ & + C_2H_2O + \text{other organic fragments} \end{aligned} \tag{2.2}$$

$$2\,{}^{\cdot}NO + O_2 \longrightarrow 2\,{}^{\cdot}NO_2 \tag{2.3}$$

$$2\,{}^{\cdot}NO_2 \rightleftharpoons N_2O_4 \tag{2.4}$$

Hydrolytic initiation

$$R{-}ONO_2 + H_2O \longrightarrow R{-}OH + HNO_3 \tag{2.5}$$

$$R{-}OH + HNO_3 \longrightarrow R{=}O + HNO_2 + H_2O \tag{2.6}$$

Propagation

$$HNO_3 + HNO_2 \rightleftharpoons N_2O_4 + H_2O \tag{2.7}$$

$$N_2O_4 \rightleftharpoons 2\,{}^{\cdot}NO_2 \tag{2.8}$$

$$R{-}OH + {}^{\cdot}NO_2 \longrightarrow {}^{\cdot}R{-}OH + HNO_2 \tag{2.9}$$

$${}^{\cdot}R{-}OH + HNO_3 \longrightarrow R{=}O + H_2O + {}^{\cdot}NO_2 \tag{2.10}$$

contrast, the low temperature hydrolytic process emphasised formation of pentaerythritol trinitrate (PETRIN) followed by side reactions with reduced likelihood of radical recombination in solution compared to in a solid , as $^{\cdot}NO_2$ would be more likely to diffuse and react elsewhere. Chin *et al.* proposed schemes for the propagation of secondary reactions initated by both the thermolysis (scheme **??**) and hydrolysis of nitrate esters (scheme **??**) [18].

(Say something about the thermolyti scheme.) Termination reactions were not emphasised in either of the schemes for these cases. The hydrolysis scheme was adapted from an earlier work by Camera *et al.* (first referenced in section 1.4) involving the nitrate ester decomposition and subsequent reactions of ethyl nitrate (where R = CH_3CH_2 for the scheme above) [12]. The original study included an expansion of the hydrolysis step (equation equ:protonation,), where the involvement of NO_2^+ was illustrated (scheme **??**

It was highlighted by Camera, that the oxidation of alcohol by nitric acid (equation 2.6) is slow and thus rate-limiting. The mechanism is likely to occur *via* a series of intermediate reactions of which the details are not known. Following the generation of nitrous

Hydrolysis scheme for ethyl nitrate

$$CH_3CH_2ONO_2 + H^+ \overset{\text{fast}}{\rightleftharpoons} CH_3CH_2ONO_2H^+ \tag{2.11}$$

$$CH_3CH_2ONO_2H^+ \overset{\text{slow}}{\rightleftharpoons} CH_3CH_2OH + {NO_2}^+ \tag{2.12}$$

$${NO_2}^+ + 2H_2O \overset{\text{fast}}{\rightleftharpoons} HNO_3 + H_3O^+ \tag{2.13}$$

acid, subsequent oxidations occur rapidly. According to Rigas *et al.*, alcohols are more susceptible to wet oxidation than esters [19]. A higher concentration of unsubstituted hydroxyl groups in the system, and therefore a fewer nitrate ester groups (or a lower degree of substitution (DOS) value), decreases overall stabililty.

Equations 2.7 - 2.10 describe a possible branched radical chain mechanism, fed by the nitrous and nitric acids produced during the hydrolysis and alchohol oxidation reactions during the initiation stage. By contrast, the propagation reactions in the branched radical chain mechanism for thermolysis are poorly characterised (equation 2.2), defined only by the observable products. This is likely due to their rapid and varied nature, rendering it difficult to follow spectroscopically.

Aellig *et al.* presented an alternative scheme for the decomposition of benzyl nitrate (R = $PhCH_2$), involving more interaction with the solvent [20]:

HNO_3 decomposition initiated

$$4HNO_3 \rightleftharpoons 4\,{}^{\cdot}NO_2 + 2H_2O + O_2 \tag{2.14}$$

$$2\,{}^{\cdot}NO_2 + H_2O \rightleftharpoons N_2O_4 + H_2O \tag{2.15}$$

$$N_2O_4 + H_2O \longrightarrow HNO_3 + HNO_2 \tag{2.16}$$

Propagation

$$R{-}OH + HNO_2 \rightleftharpoons R{-}ONO + H_2O \tag{2.17}$$

$$R{-}ONO \longrightarrow R{=}O + HNO \tag{2.18}$$

$${}^{\cdot}NO_2 + HNO \longrightarrow HNO_2 + {}^{\cdot}NO \tag{2.19}$$

$$2\,{}^{\cdot}NO + O_2 \longrightarrow 2\,{}^{\cdot}NO_2 \tag{2.20}$$

Termination

$$2HNO \longrightarrow HON{=}NOH \tag{2.21}$$

$$HON{=}NOH \longrightarrow N_2O + H_2O \tag{2.22}$$

Both the Camera/Chin and Aellig schemes above produce final end products observed in the decomposition of NC. In particular, Aellig's scheme accounts for the production of N_2O, which forms a significant part of the decomposition eluent [21]. Whilst the schemes do not a propose an exhaustive description of the full spectrum of reactions that take place in the NC matrix during its slow ageing, the early stage reactions of the key species responsible for decomposition are encapsulated.

It is widely agreed that first-stage decomposition follows a first-order process (or pseudo-first order, with respect to hydrolysis reactions). A number of studies observe catalytic rate of decay for the longer-term aging processes. Dauerman [22] observed that when NC was treated with NO_2 gas before heating, the time required for sample ignition halved. He suggested that the NO_2 adsorbed onto the surface acted as a catalysing agent.

Neutral and alkaline hydrolysis reactions follow a pseudo-first order process, however it has been suggested that the presence of acid facilitates a catalytic rate of degradation after an initial incubation period. Multiple studies have addressed the decomposition reactions of nitrate esters following the initial scission of the nitrate group [10, 12, 23, 14, 13] In their work looking into the atmospheric reactions methyl nitrate methylperoxy nitrate Arenas (2007) suggested it was possible for the homolytic denitration reaction of methyl nitrate to share a common peroxy intermediate with the peroxide. This could account for some of the different/lower order NO_x generated (just ˙NO, tbh, or maybe perhaps how NO3 may get generated?).

In this section, secondary and extended reaction schemes for the low temperature ageing of NC are explored. Decompostition pathways defined by Chin, Camera and Aellig *et al.* are probed to determine the reactions responsible for the experimentally observed degradation products. The reactions found to be energetically feasible from the proposed routes will be scrutinised to determine whether an autocatalytic pathway can be formed from the thermodynamically validated reaction schemes.

2.2 Methodology

The schemes proposed by Chin, Camera and Aellig *et al.* were used to construct possible degradation routes for NC with the products of homolytic fission, elimination of HNO_2 and acid hydrolysis used as the starting point. Pathways were constructed based on propagation of the given reactions in a step-wise fashion; subsequent reactions were dependent on the products generated in preceding steps. An abundance of water and oxygen were assumed

present in the system, attributed to air exposure under the wetted storage conditions of NC. Unsubsitutued alcohol moieties (R-OH) were also presumed available, due to incomplete nitration during the synthesis of NC [24], and re-generation following denitration *via* hydrolysis. The schemes were modelled with both ethyl nitrate and the NC monomer. Free energies of reaction (Δ G) were used to determine the feasibility of each reaction.

2.2.1 Computational details

All geometry optimisations were conducted in G09, using the ωB97X-D and B3LYP functionals. Optimisations and thermochemistry calculations were performed to the level of 6-31+G(2df,p) with tight convergence criteria (table **??**). Calculations were performed in both vacuum and with PCM to introduce implicit solvent effects. Chemical species were constructed using Gauss View 5.0.8 (GView) and for molecules of more than 3 atoms, the "Clean" function was used to re-order atoms to a preliminary starting geometry. Energies of optimised structures were checked against values listed on NIST Computational Chemistry Comparison and Benchmark Database [25] if analogous molecules to a similar level of theory were available.

2.3 Results and Discussion

Simplified schemes for the ageing reactions of NC beginning from homolytic fission, elimination of HNO_2 or acid hydrolysis are illustrated in schemes 2.1 - 2.3.

When starting with the products of homolytic fission, a branched radical chain mechanism dominates. $^{\cdot}NO_2$ and HNO_2 were consumed and regenerated, supporting the theory that these may be species contributing to the observed autocatalytic rate of decomposition, following a first-order rate induction period [5, 6, 7]. For all schemes, R=O and N_2O were terminating species, which may go on to participate in wider reactions outside the scope of the proposed reactions. Table **??** shows the energies for the reactions in all schemes, for both ethyl nitrate and the NC monomer.

Still to mention:

- Describe the other two schemes

- Describe the energies in the table - what are the experimental energies for them, and how do my values compare?

- Discuss why some of the values may be positive.

- Include enthalpies of reaction, zero point energies, and any experimental proxies I can find

for the reaction enthalpies too.

NOTE: ZPE energy correction means that you REMOVE the ZPE, so that you only compare the actual energy available for the reaction. - Look a little more into (pics of the species / reactions, etc on a few specific funny cases, and explain what you see - ie. different resulst for different funcitonals. - explain why -

Table 2.1: Energies of nitrate ester decomposition reactions proposed by Camera [12], Chin [18] and Aellig [20]. R = CH_3CH_2 for ethyl nitrate, and R = $(H_3CO)_2C_6H_9O_3$ (bi-methoxy capped glucopyraonse monomer unit).

Reaction	ΔG_r /kcal mol^{-1}			
	ωB97X-D	PCM	B3LYP	PCM
$N_2O_4 + H_2O \longrightarrow HNO_3 + HNO_2$	2.25	1.85	5.13	4.18
$N_2O_4 \rightleftharpoons 2\,^{\cdot}NO_2$	0.12	1.46	−0.54	−0.16
Radical reactions				
$2\,^{\cdot}NO_2 \rightleftharpoons N_2O_4$	−0.12	−1.31	0.54	0.16
$^{\cdot}NO_2 + HNO \longrightarrow HNO_2 + {}^{\cdot}NO$	−28.22	−28.67	−27.33	−27.63
$2\,^{\cdot}NO + O_2 \longrightarrow 2\,^{\cdot}NO_2$	−20.77	−21.97	−21.16	−22.16
$2^{\cdot}NO + O_2 \longrightarrow 2^{\cdot}NO_2$	−59.89	−60.47	−60.47	−61.00
Acid reactions				
$HNO_3 + HNO_2 \rightleftharpoons N_2O_4 + H_2O$	−2.25	−1.85	−5.13	−4.18
$4\,HNO_3 \rightleftharpoons 4\,NO_2 + 2\,H_2O + O_2$	53.35	58.36	42.61	46.94
$2\,HNO \longrightarrow HON{=}NOH$	−38.97	−39.72	−36.63	−37.41
$HON{=}NOH \longrightarrow N_2O + H_2O$	−48.08	−48.18	−50.55	−50.75
Ionic reactions				
$NO_2^+ + 2\,H_2O \rightleftharpoons HNO_3 + H_3O^+$	−0.90	−1.34	1.77	2.46
Ethyl nitrate (R = CH_3CH_2)				
$R{-}ONO_2 + H_2O \longrightarrow R{-}OH + HNO_3$	4.56	5.24	4.00	4.86
$R{-}OH + HNO_3 \longrightarrow R{=}O + HNO_2 + H_2O$	−34.06	−38.43	−37.59	−41.77
$R{-}OH + {}^{\cdot}NO_2 \longrightarrow {}^{\cdot}R{-}OH + HNO_2$	16.38	13.92	15.89	13.70
$^{\cdot}R{-}OH + HNO_3 \longrightarrow R{=}O + H_2O + {}^{\cdot}NO_2$	−50.44	−52.35	−53.48	−55.47
$R{-}OH + HNO_2 \rightleftharpoons R{-}ONO + H_2O$	−3.21	−3.28	−2.64	−2.95
$R{-}ONO \longrightarrow R{=}O + HNO$	−1.50	−5.82	−4.37	−8.50
NC monomer (R = $(H_3CO)_2C_6H_9O_3$)				
$R{-}ONO_2 + H_2O \longrightarrow R{-}OH + HNO_3$	0.68	5.63	0.61	−0.70
$R{-}OH + {}^{\cdot}NO_2 \longrightarrow {}^{\cdot}R{-}OH + HNO_2$	14.71	11.15	13.03	23.21
$^{\cdot}R{-}OH + HNO_3 \longrightarrow R{=}O + H_2O + {}^{\cdot}NO_2$	−51.44	−49.49	−54.75	−56.37
$R{-}OH + HNO_2 \rightleftharpoons R{-}ONO + H_2O$	−4.43	−7.30	−4.31	−0.18
$R{-}ONO \longrightarrow R{=}O + HNO$	−2.93	−1.71	−6.82	−11.21

Due to the availability of oxygen sites on the ethyl nitrate molecule, the optimal site for protonation was determined for inclusion in the reaction scheme for the first stage of

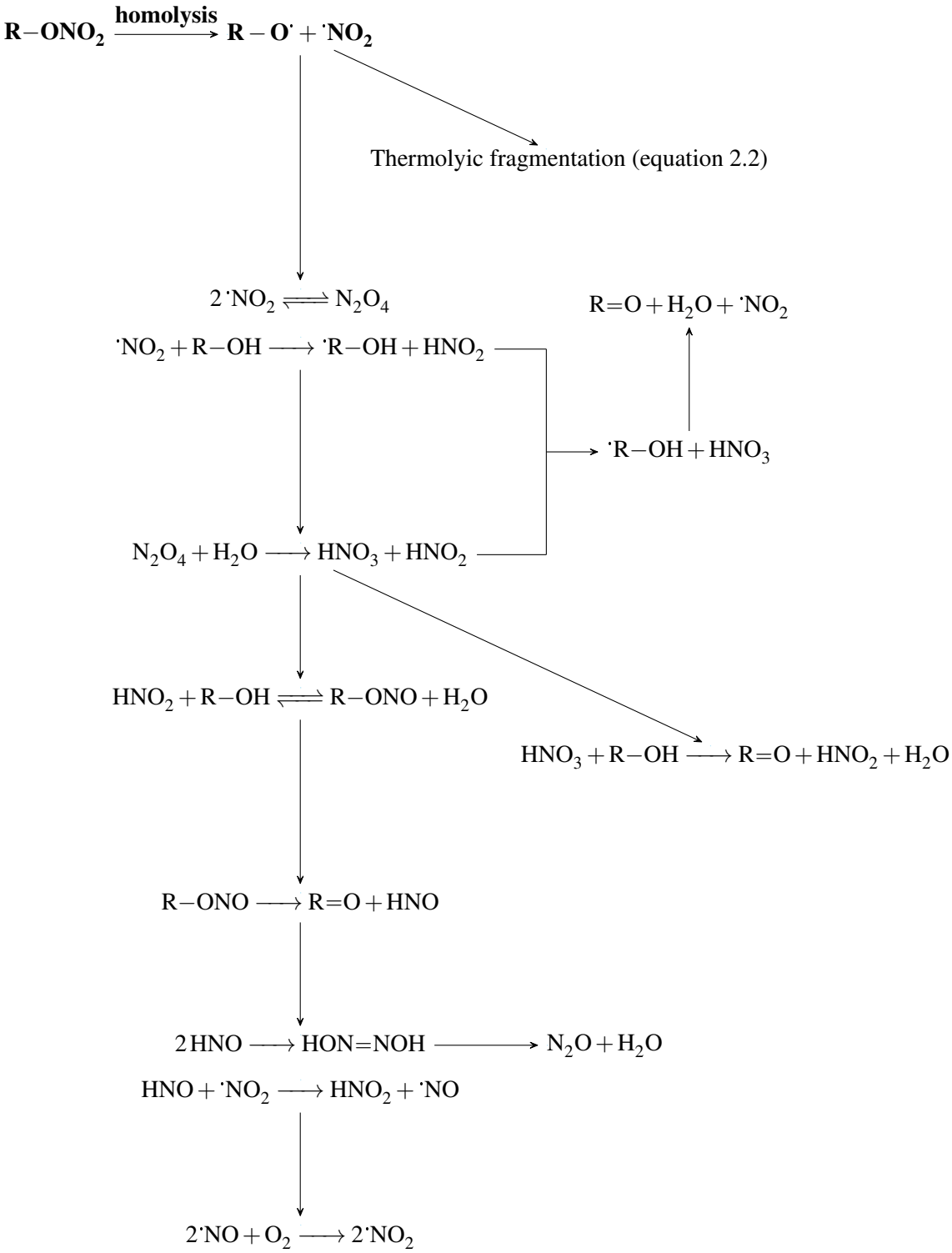

Scheme 2.1: Proposed degradation pathway starting from the homolytic fission of the nitrate ester, derived from the schemes presented by Camera [12] and Aellig[20].

Table 2.2: Free energies of protonation for each oxygen site on ethyl nitrate.

Protonated site		ΔG_r /kCal mol^{-1}			
		ωB97X-D	PCM	B3LYP	PCM
Terminal (upper)	$CH_3CH_3ONO_2H^+$	−12.28	8.82	−13.78	5.63
Terminal (lower)	$CH_3CH_3ONO_2H^+$	−9.48	9.46	−11.13	5.65
Bridging	$CH_3CH_3O(H^+)NO_2$	−9.32	9.06	−15.31	6.67

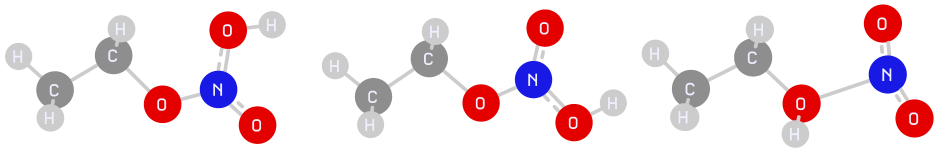

(a) Upper terminal oxgen. Bond(O–NO_2): 1.28 Å

(b) Lower terminal oxgen. Bond(O–NO_2): 1.28 Å

(c) Bridging oxgen. Bond(O–NO_2): 1.98 Å

Figure 2.4: Optimised geometries of the possible protonation sites on ethyl nitrate.

hydrolysis. Table 2.2 shows the protonation energies for the three different oxygen sites on ethyl nitrate. Despite the upper terminal oxygen possessing the most thermodynamically favourable energy of protonation, inspection of the reaction geometries shows that the bridging structure most resembles that expected for the liberation of the NO_2^+ group at the next step. Though appearing less thermodynamically favourable when compared to protonation at the terminal upper oxygen site, the higher energy of reaction likely arises from the instability of the protonated complex. The elongation of the O–NO_2 bond allows to stabilisation of the proton at the bridging site, such that the departure of NO_2^+ is easily facilitated. Subsequent calculation involving the energy of the protonated ethyl nitrate will employ the values associated with the protonated bridging site.

For the decomposition of HNO_3 to $.NO_2$, $2H_2O$ and O_2, Aellig prescribes the use of an amberlyst catalyst (amberlyst-15).

In case I decide to look at any NMR for the degradatino products, and need to explain how NMR values are derived compuationally; [16]. (And also teh Gaussian textbok)

2.4 Summary

Map of the possible reactions, linking to

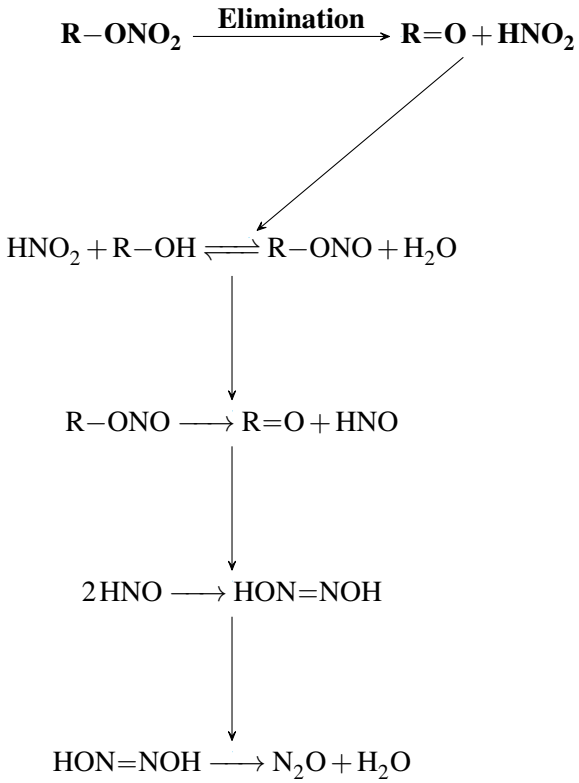

Scheme 2.2: Proposed degradation pathway starting from the elimination of HNO_2 from a nitrate ester, derived from the schemes presented by Camera [12] and Aellig[20].

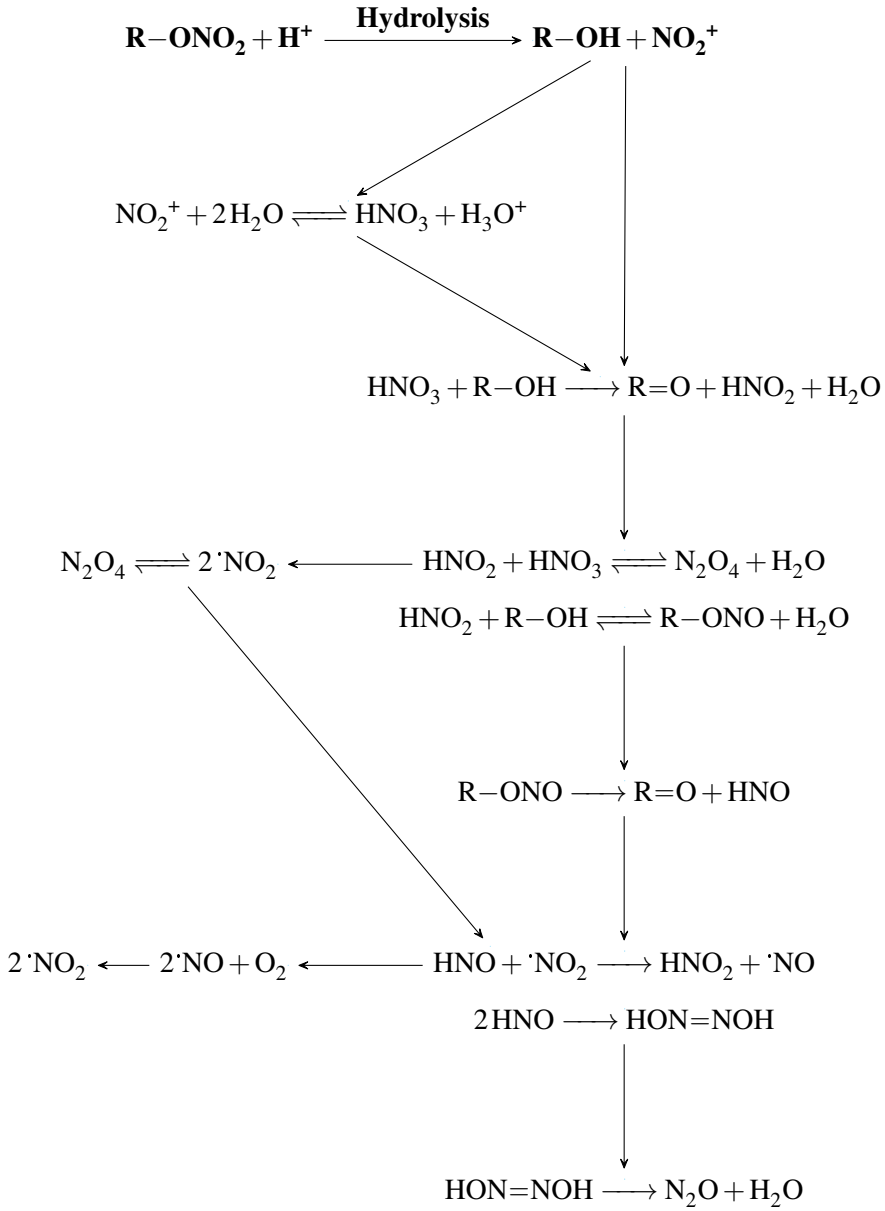

Scheme 2.3: Proposed degradation pathway starting from the acid hydrolysis of a nitrate ester, derived from the schemes presented by Camera [12] and Aellig[20].

Bibliography

[1] Jimmie C. Oxley. A survey of the thermal stability of energetic materials, jan 2003.

[2] M F Foltz. Aging of pentaerythritol tetranitrate (PETN). *LLNL-TR-415057, Lawrence Livermore National Laboratory, Livermore, CA, USA*, apr 2009.

[3] Mohammed Moniruzzaman, John M. Bellerby, and Manfred A. Bohn. Activation energies for the decomposition of nitrate ester groups at the anhydroglucopyranose ring positions C2, C3 and C6 of nitrocellulose using the nitration of a dye as probe. *Polymer Degradation and Stability*, 102:49–58, apr 2014.

[4] Roman V. Tsyshevsky, Onise Sharia, and Maija M. Kuklja. Thermal Decomposition Mechanisms of Nitroesters: Ab Initio Modeling of Pentaerythritol Tetranitrate. *The Journal of Physical Chemistry C*, 117(35):18144–18153, sep 2013.

[5] I. Rodger and J. D. Mcirvine. The decomposition of spent PETN nitration acids. *The Canadian Journal of Chemical Engineering*, 41(2):87–90, apr 1963.

[6] Torbjórn Lindblom. Reactions in stabilizer and between stabilizer and nitrocellulose in propellants. *Propellants, Explosives, Pyrotechnics*, 27(4):197–208, sep 2002.

[7] Hermann N. Volltrauer and Arthur Fontijn. Low-temperature pyrolysis studies by chemiluminescence techniques real-time nitrocellulose and PBX 9404 decomposition. *Combustion and Flame*, 41:313–324, jan 1981.

[8] M. Edge, N.S. Allen, M. Hayes, P.N.K. Riley, C.V. Horie, and J. Luc-Gardette. Mechanisms of deterioration in cellulose nitrate base archival cinematograph film. *European Polymer Journal*, 26(6):623–630, jan 1990.

[9] Mª Ángeles Fernández de la Ossa, María López-López, Mercedes Torre, and Carmen García-Ruiz. Analytical techniques in the study of highly-nitrated nitrocellulose. *TrAC Trends in Analytical Chemistry*, 30(11):1740–1755, dec 2011.

[10] John W. Baker and D. M. Easty. Hydrolytic decomposition of esters of nitric acid. Part I. General experimental techniques. Alkaline hydrolysis and neutral solvolysis of methyl, ethyl, isopropyl, and tert.-butyl nitrates in aqueous alcohol. *Journal of the Chemical Society (Resumed)*, 1952(0):1193–1207, 1952.

[11] N. Binke, L. Rong, Y. Zhengquan, W. Yuan, Y. Pu, Hu Rongzu, and Y. Qingsen. Studies on the Kinetics of the First Order Autocatalytic Decomposition Reaction of Highly Nitrated Nitrocellulose. *Journal of Thermal Analysis and Calorimetry*, 58(2):403–411, 1999.

[12] E. Camera, G. Modena, and B. Zotti. On the Behaviour of Nitrate Esters in Acid Solution. II. Hydrolysis and oxidation of nitroglycol and nitroglycerin. *Propellants, Explosives, Pyrotechnics*, 7(3):66–69, jun 1982.

[13] K. S. Hu, A. I. Darer, and M. J. Elrod. Thermodynamics and kinetics of the hydrolysis of atmospherically relevant organonitrates and organosulfates. *Atmospheric Chemistry and Physics*, 11(16):8307–8320, aug 2011.

[14] V. G. Matveev and G. M. Nazin. Stepwise Degradation of Polyfunctional Compounds. *Kinetics and Catalysis*, 44(6):735–739, nov 2003.

[15] S. Miertuš, E. Scrocco, and J. Tomasi. Electrostatic interaction of a solute with a continuum. A direct utilizaion of AB initio molecular potentials for the prevision of solvent effects. *Chemical Physics*, 55(1):117–129, feb 1981.

[16] Vladimir M. Gun'ko, Waldemar Tomaszewski, Tetyana V. Krupska, Konstantin V. Turov, Roman Leboda, and Vladimir V. Turov. Interfacial behavior of water bound to nitrocellulose containing residual nitric and sulfuric acids. *Central European Journal of Chemistry*, 12(4):509–518, jan 2014.

[17] M. Moniruzzaman and J.M. Bellerby. Use of UV-visible spectroscopy to monitor nitrocellulose degradation in thin films. *Polymer Degradation and Stability*, 93(6):1067–1072, jun 2008.

[18] Anton Chin, Daniel S. Ellison, Sara K. Poehlein, and Myong K. Ahn. Investigation of the Decomposition Mechanism and Thermal Stability of Nitrocellulose/Nitroglycerine Based Propellants by Electron Spin Resonance. *Propellants, Explosives, Pyrotechnics*, 32(2):117–126, apr 2007.

[19] Fotis Rigas, Ioannis Sebos, and Danae Doulia. Safety Charts Simulation of Nitroglycerine/Nitroglycol Spent Acids via Chemical Reaction Kinetics. *Industrial and Engineering Chemistry Research*, 36(12):5068–5073, 1997.

[20] Christof Aellig, Christophe Girard, and Ive Hermans. Aerobe Alkoholoxidation mithilfe von HNO3. *Angewandte Chemie*, 123(51):12563–12568, dec 2011.

[21] S. J. Buelow, D. Allen, G. K. Anderson, F. L. Archuleta, and J. H. Atencio. Destruction of Energetic Materials in Supercritical Water. Technical report, AIR FORCE RESEARCH LABORATORY, 2002.

[22] L. Dauerman and Y. A. Tajima. Thermal decomposition and combustion of nitrocellulose. *AIAA Journal*, 6(8):1468–1473, aug 1968.

[23] E. Camera, G. Modena, and B. Zotti. On the behaviour of nitrate esters in acid solution. III. Oxidation of ethanol by nitric acid in sulphuric acid. *Propellants, Explosives, Pyrotechnics*, 8(3):70–73, jun 1983.

[24] Frank E. Wolf. Alkaline Hydrolyis Conversion of Nitrocellulose Fines. Technical Report October, Badger Army Ammunition Plant, oct 1997.

[25] Russell D. Johnson III. NIST Computational Chemistry Comparison and Benchmark Database NIST Standard Reference Database Number 101, 2018.